Tan et al. Nanoscale Research Letters (2018) 13:334
https://doi.org/10.1186/s11671-018-2756-2

Nanoscale Research Letters

NANO EXPRESS Open Access

Influence of Quantum-Well Width on the Electroluminescence Properties of AlGaN Deep Ultraviolet Light-Emitting Diodes at Different Temperatures

Shuxin Tan[1], Jicai Zhang[2,4*], Takashi Egawa[3*], Gang Chen[4], Xiangdong Luo[1], Ling Sun[1] and Youhua Zhu[1]

Abstract

The influence of quantum-well (QW) width on electroluminescence properties of AlGaN deep ultraviolet light-emitting diodes (DUV LEDs) was studied at different temperatures. The maximum external quantum efficiency (EQE) ratios of LED with 3.5 nm QW to that with 2 nm increased from 6.8 at room temperature (RT) to 8.2 at 5 K. However, the ratios for LED with 3.5 nm QW to that with 5 nm QW decreased from 4.8 at RT to 1.6 at 5 K. The different changes of EQE ratios were attributed to the decrease of non-radiative recombination and the increase of volume of the active region. From theoretical analysis, the LED with 2-nm wells had a shallowest barrier for electron overflow due to the quantum-confined effect, whereas the LED with 5-nm wells showed the least overlap of electron and hole due to the large internal field. Therefore, the LED with 3.5 nm QW had the highest maximum EQE at the same temperature. As temperature decreased, the current for maximum EQE decreased for all the LEDs, which was believed to be due to the increase of electron which overflowed out of QWs and the decrease of hole concentration. The results were helpful for understanding the combination of polarization effect and electron overflow in DUV LEDs.

Keywords: Deep ultraviolet light-emitting diodes, AlGaN, External quantum efficiency, Electroluminescence, Low temperature

Background

AlGaN-based deep ultraviolet light-emitting diodes (DUV LEDs) can be widely used in the fields of solid-state lighting, medicine, biochemistry, and so on. Therefore, more and more efforts have been devoted to improve the crystal quality of the materials [1–4], the p-type doping techniques, and the optimization of the device structures [5–9]. Miyake et al. demonstrated that the AlN crystal quality can be improved significantly by high-temperature annealing [3]. By increasing the growth temperature, Sun et al. obtained high-quality AlN thick films on sapphire [2]. Recently, Jiang et al. studied the defect evolution in AlN homoepitaxial growth [1]. Their results contributed to the understanding of the AlN homoepitaxy mechanism and provided the critical techniques for improving the crystal quality. In addition, many methods were proposed to improve the light extraction, such as photonic crystals and nanostructures and surface plasmon [10–12]. In the past decades, a great progress has been obtained for this kind of LED, which was reviewed overall by Li et al. [13]. Nevertheless, the performance of the devices is still far from the practical application due to the low external quantum efficiency. It is well known that group III nitrides have wurtzite structures, in which the large spontaneous and piezoelectric fields will result in the tilted band diagram. These tilted bands had great influence on group-III nitride-based devices, such as LED, LD [14, 15], and UV detectors [16, 17]. Hirayama et al. reported the influence of quantum-well (QW) width on the photoluminescence (PL) properties in AlGaN-based single-QW DV LEDs [18]. They found that the LEDs

* Correspondence: jczhang@mail.buct.edu.cn; egawa.takashi@nitech.ac.jp
[2]Department of Physics, College of Science, Beijing University of Chemical Technology, 15 East Road, Beisanhuan, Beijing 100029, China
[3]Research Center for Nano-Device and System, Nagoya Institute of Technology, Gokiso-cho, Showa-ku, Nagoya 466-8555, Japan
Full list of author information is available at the end of the article

Springer Open
© The Author(s). 2018 **Open Access** This article is distributed under the terms of the Creative Commons Attribution 4.0 International License (http://creativecommons.org/licenses/by/4.0/), which permits unrestricted use, distribution, and reproduction in any medium, provided you give appropriate credit to the original author(s) and the source, provide a link to the Creative Commons license, and indicate if changes were made.

with QW width of 1.5–1.7 nm exhibited a higher luminescence and the PL intensity decreased when the QW width was less than 1.5 nm, which was attributed to an increase of nonradiative recombination on the heterointerfaces. In this work, we fabricated DUV LEDs with different quantum-well (QW) width and studied the influence of the QW width and temperature on the electroluminescence (EL) properties. We found the LEDs with QW width of 3.5 nm exhibited the highest maximum external quantum efficiency (EQE). As the temperature decreased, the current for the maximum EQE decreased for all the LEDs, which was believed to be due to the decrease of hole concentration and the increase of overflowed electron current.

Methods

The LEDs were grown by metal-organic chemical vapor deposition on (0001)-sapphire substrate using a 1.0-μm AlN buffer layer followed by a 0.5-μm-thick undoped $Al_{0.6}Ga_{0.4}N$ and a 1.0-μm-thick n-$Al_{0.6}Ga_{0.4}N$ template. The dislocation density of the template is around 6×10^9 cm^{-2} measured by transmission electron microscopy. Then $Al_{0.49}Ga_{0.51}N/Al_{0.58}Ga_{0.42}N$ multiple QWs (MQWs) were grown as active regions. The thickness of the barriers was 5.0 nm. p-$Al_{0.3}Ga_{0.7}N$ (25 nm)/$Al_{0.6}Ga_{0.4}N$ (25 nm) was used as p-type layers. Finally, a 200-nm p-GaN contact layer was deposited. Based on the above structure, three samples, named LEDs A, B, and C, were grown with QW width of 2.0, 3.5, and 5.0 nm, respectively.

500 μm × 500 μm square geometry *p-n* junction devices were fabricated using standard lithographic techniques to define the feature and reactive ion etching to expose the *n*-$Al_{0.6}Ga_{0.4}N$ Ohmic-contact layer. n-type Ohmic contacts of Ti/Al/Ni/Au (15/80/12/60 nm) were deposited by electron-beam evaporation and annealed with a rapid thermal annealing system at 900 °C for 30 s in nitrogen ambience. For transparent *p*-contacts, Ni/Au (6/12 nm) layers were electron-beam deposited and annealed in air ambience at 600 °C for 3 min. The device was completed with the deposition of Ni/Au (5/60 nm) *p* contact. The EL spectrum was measured from 5 K to room temperature (RT) using Jonin Yvon's Symphony UV-enhanced liquid nitrogen-cooled charge-coupled device detector. To avoid the influence of thermal heating effect [19], the pulse injection with 1 μs current pulse at 0.5% was used in the EL measurements.

Results and Discussion

Figure 1a shows the EL spectra measured at room temperature (RT) for LEDs A, B, and C under direct current of 100 mA, in which all the spectra were normalized to the band-to-band emission. The EL peaks for LEDs A, B, and C were around 261, 265, and 268 nm, respectively. Obviously, the EL peak showed a redshift as the QW width increased. In addition, it should be noticed that a weak parasitic peak around 304 nm existed in the EL spectrum in LED A, which was clarified to be related with electron overflow [20]. Figure 1b shows the relative EQE as a function of pulse current for all the LEDs. All the values were normalized to the maximum EQE of LED B. The maximum EQE of LED B was about 6.8 and 4.8 times than those of LEDs A and C, respectively.

In order to understand the reason, APSYS was used to simulate the energy levels and wave functions of carriers. Figure 2a–c shows the band structures, the ground state level, and carrier wave functions in one QW under current of 100 mA for LEDs A, B, and C, respectively. Due to the large internal field induced by the polarization effect and the applied forward bias, the band structure of QW showed an inclined shape and the spatial overlapping of wave functions of electrons and holes became less as the QW width increased due to the quantum-confined Stark effect (QCSE). The energy gap of the ground states for LEDs A, B, and C were 4.733, 4.669, and 4.637 eV, respectively, which coincided well with the emission wavelength as shown in Fig. 1a. In addition, it should be noticed that the confined ability of carriers by the QWs decreased as the QW width

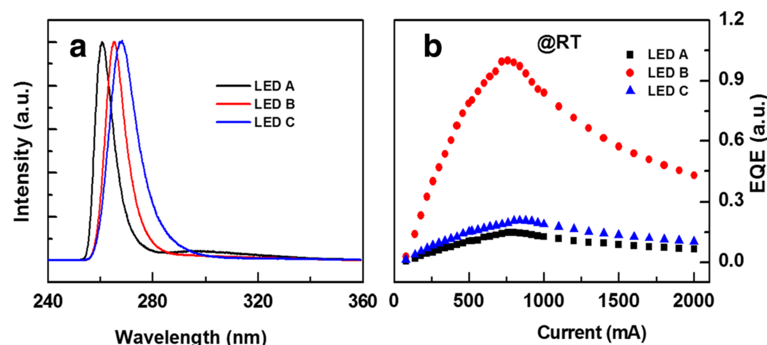

Fig. 1 **a** The RT EL spectra for LEDs A, B, and C under direct current of 100 mA. All the spectra were normalized to the band-to-band emission. **b** The relative EQE as a function of pulse current

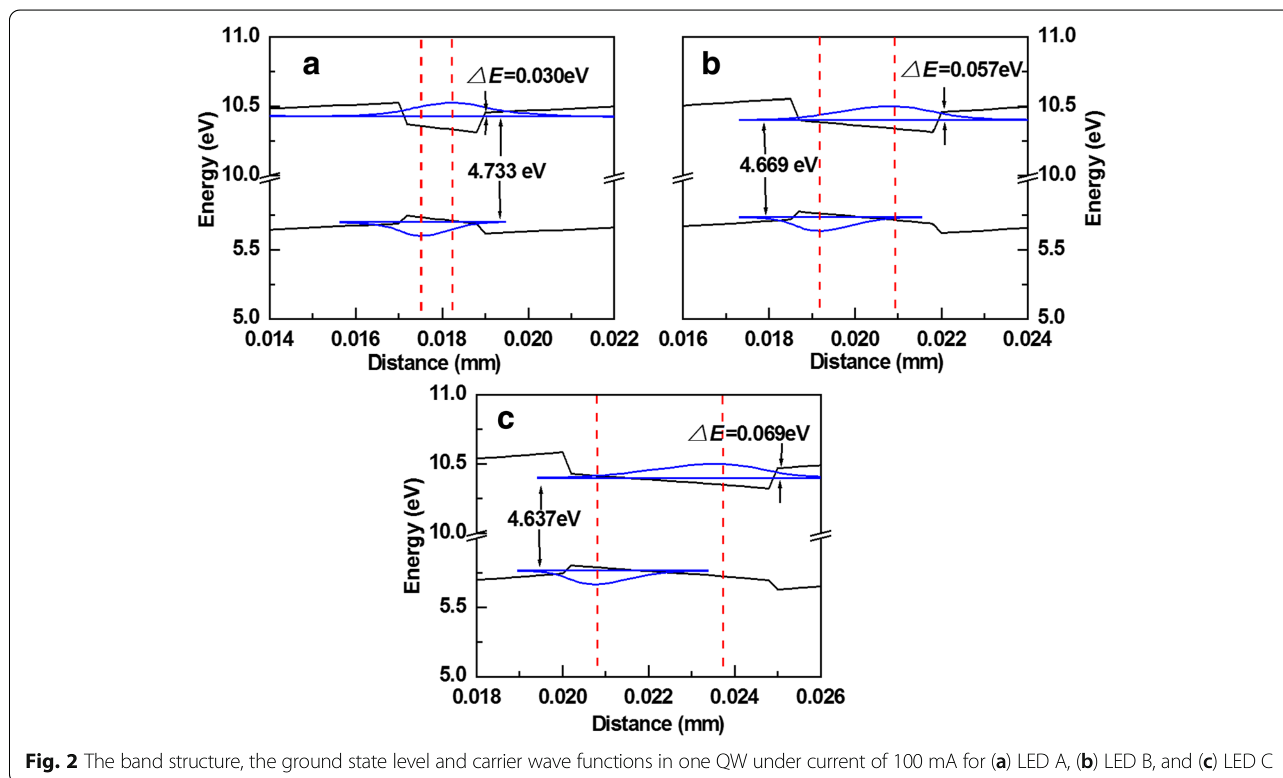

Fig. 2 The band structure, the ground state level and carrier wave functions in one QW under current of 100 mA for (**a**) LED A, (**b**) LED B, and (**c**) LED C

decreased. The quantum-confined effect resulted in the increase of the ground state level as the QW width decreased. The values of barrier height were 0.030, 0.057, and 0.069 eV for LEDs A, B, and C, respectively. Therefore, the EQE of LED A was less than that of LED B due to the electron current overflow, which could be confirmed by the obvious parasitic peak shown in Fig. 1a. Though LED C had the highest barrier for electron overflow in all the devices, its EQE was still less than that of LED B due to the QCSE.

The EQE at low temperature was measured to evaluate the device performance. Figure 3a shows the relative EQE measured at 5 K. All the values were normalized to the maximum EQE of LED B. Obviously, the injection current for the maximum EQE decreased significantly compared to those at RT for all the devices. The maximum EQE of LED B was about 8.2 and 1.6 times than those of LEDs A and C, respectively. The current-dependent EQE were measured at different temperature. Figure 3b shows the current-dependent relative EQE at different temperature for LED B. All the values were normalized to the maximum EQE at 10 K. It can be seen that the current for the maximum EQE decreased as the temperature decreased. The same phenomenon was found for all three LEDs. It was well known that in bulk materials the hole concentration

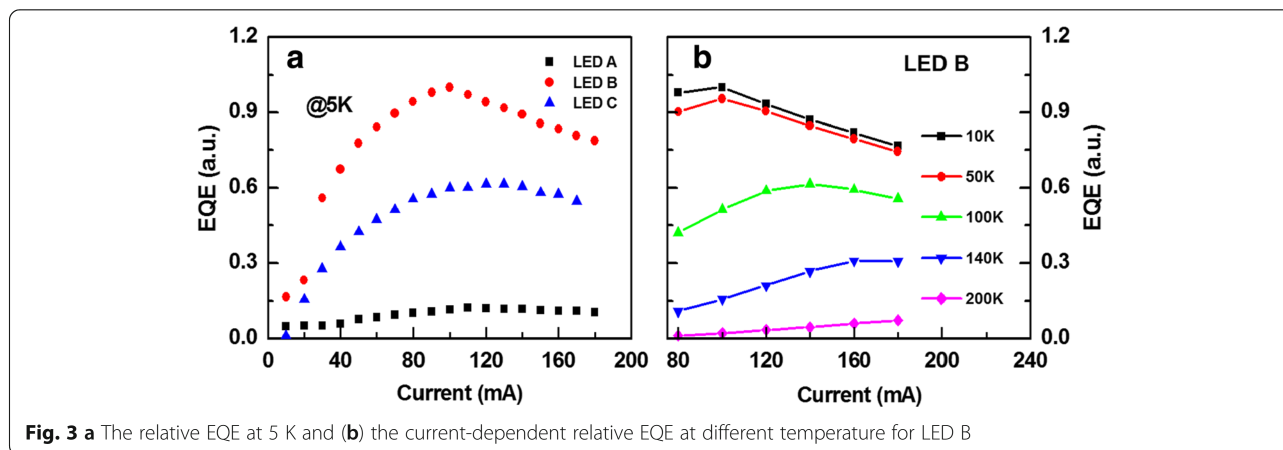

Fig. 3 **a** The relative EQE at 5 K and (**b**) the current-dependent relative EQE at different temperature for LED B

would decrease rapidly with decreasing temperature due to the high ionization energy of Mg in p-AlGaN. In our structure, it was demonstrated that the hole concentration also decreased as the temperature decreased [21]. We also simulated the hole distribution at different temperature. Figure 4 shows the hole concentrations in active region at 100 and 300 K for LED B under the injection of 100 mA. Obviously, the hole concentration decreased as the temperature decreased. In addition, the electron current overflowed out of QWs can be expressed as [22].

$$J_{\text{overflow}} = D\left(\frac{\Delta E}{kT}\right)^3 qBl$$

where D is a constant, ΔE is the difference of Fermi level and band edge of quantum wells, K is the Boltzmann constant, T is the temperature, q is the electron charge, B is the bimolecular radiative recombination coefficient, and l is the thickness of MQWs. For a certain LED, the contribution of variation of ΔE to J_{overflow} could be neglected compared to that of T as the temperature decreased. Therefore, the J_{overflow}increased significantly at 5 K compared to that of RT, which was believed to be the main reason for the decrease of injection current at which the maximum EQE reached. The J_{overflow} decreased as the temperature increased, resulting in the increase of injection current for the maximum EQE, as shown in Fig. 3b. At low temperature, the internal efficiency would increase due to the freeze-out of nonradiative centers, such as the dislocations, which was beneficial to LED C with the largest volume of active region. This was the most possible reason why the EQE ratio of LED B to LED C decreased at 5 K compared to that at RT. Similarly, the EQE ratio of LED B to LED A increased at 5 K compared to that at RT.

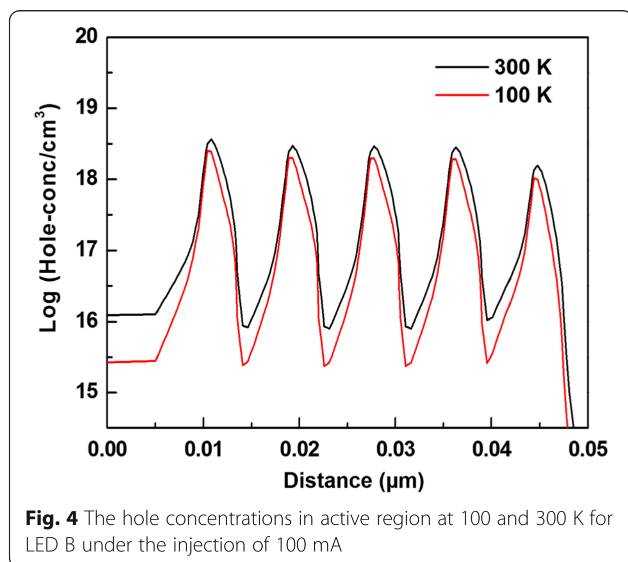

Fig. 4 The hole concentrations in active region at 100 and 300 K for LED B under the injection of 100 mA

Conclusions

We studied the influence of QW width on EL properties of AlGaN DUV LEDs at different temperatures. The EL spectra showed a redshift as the QW width increased. The maximum EQE for LED with QW width of 3.5 nm was about 6.8 and 4.8 times than those of 2 and 5 nm at RT, respectively. However, these values changed to be 8.2 and 1.6 at 5 K, respectively. The different changes of maximum EQE ratios were attributed the decrease of non-radiative recombination and the increase of volume of the active region. From the theoretical analysis, the LED with 2-nm wells showed a shallowest barrier for electron overflow due to the quantum-confined effect, whereas the LED with 5-nm wells showed a least overlap of electron and hole due to the large internal field. Therefore, the LED with 3.5 nm QWs showed the highest maximum EQE. As the temperature decreased, the current for the maximum EQE decreased for all LEDs, which was believed to be due to the increase of electron overflowed out of QWs and the decrease of hole concentration. The maximum EQE for LED with QW width of 3.5 nm was about 8.2 and 1.6 times of those of 2 and 5 nm at 5 K, respectively, which was believed to be due to the decrease of non-radiative recombination centers and the increase of volume of active region.

Abbreviations

DUV LEDs: Deep ultraviolet light-emitting diodes; EL: Electroluminescence; EQE: External quantum efficiency; MQW: Multiple quantum well; PL: Photoluminescence; QCSE: Quantum-confined Stark effect; QW: Quantum well; RT: Room temperature

Acknowledgements

The authors of JCZ and ST would like to extend their gratitude to Professor B. S. Zhang and Associate Professors K. Fu and G. H. Yu (Suzhou Institute of Nano-tech and Nano-bionics, CAS,) for their kind help during the simulation and fruitful discussions.

Funding

This work was partly supported by the National Natural Science Foundation of China (No. 61474133, 61504071), Beijing Municipal Natural Science Foundation (4182046), the research project of Beijing University of Chemical Technology (YY1701, buctrc201802), and the Natural Science Foundation of Nantong University (Grant No.03081003).

Availability of Data and Materials

The datasets used and/or analyzed during the current study are available from the corresponding author on reasonable request.

Authors' Contributions

ST did the simulations and wrote and revised the manuscript. JCZ and TE supervised the research work and revised the manuscript. GC repeated the simulations. XDL and LS contributed to discussion of the results and manuscript revision. YHZ contributed to the device process. All authors read and approved the final manuscript.

Competing Interests

The authors declare that they have no competing interests.

Publisher's Note

Springer Nature remains neutral with regard to jurisdictional claims in published maps and institutional affiliations.

Author details
[1]School of Electronics and Information, Nantong University, 9 Seyuan Road, Nantong 226019, China. [2]Department of Physics, College of Science, Beijing University of Chemical Technology, 15 East Road, Beisanhuan, Beijing 100029, China. [3]Research Center for Nano-Device and System, Nagoya Institute of Technology, Gokiso-cho, Showa-ku, Nagoya 466-8555, Japan. [4]Suzhou Institute of Nano-Tech and Nano-Bionics, CAS, 398 Ruoshui Road, SEID, SIP, Suzhou 215123, China.

Received: 29 August 2018 Accepted: 14 October 2018
Published online: 23 October 2018

References

1. Jiang K, Sun X, Ben J, Jia Y, Liu H, Wang Y, Wu Y, Kai C, Li D (2018) The defect evolution in homoepitaxial AlN layers grown by high-temperature metal–organic chemical vapor deposition. CrystEngComm 20:2720–2728
2. Sun M, Zhang J, Huang J, Li X, Wang L, Liu X, Wang J, Xu K (2016) Influence of thickness on strain state and surface morphology of AlN grown by HVPE. J Semicond 37(12):123001
3. Miyake H, Lin C-H, Tokoro K, Hiramatsu K (2016) Preparation of high-quality AlN on sapphire by high-temperature face-to-face annealing. J Cryst Growth 456:155–159
4. Kim H, Yoon HJ, Choi BJ (2018) Thickness dependence on interfacial and electrical properties in atomic layer deposited AlN on c-plane GaN. Nanoscale Res Lett 13:232
5. Hirayama H, Maeda N, Fujikawa S, Toyoda S, Kamata N (2014) Recent progress and future prospects of AlGaN-based high-efficiency deep-ultraviolet light-emitting diodes. Jap J Appl Phys 53:100209
6. Kinoshita T, Obata T, Yanagi H, Inoue S (2013) High p-type conduction in high-Al content Mg-doped AlGaN. Appl Phys Lett 102:012105
7. Li S, Ware M, Wu J, Minor P, Wang Z, Wu Z, Jiang Y, Salamo GJ (2012) Polarization induced pn-junction without dopant in graded AlGaN coherently strained on GaN. Appl Phys Lett 101:122103
8. S, Zhang T, Wu J, Yang Y, Wang Z, Wu Z, Chen Z, and Jiang YPolarization induced hole doping in graded $Al_xGa_{1-x}N$ (x = 0.7 ~1) layer grown by molecular beam epitaxy Appl Phys Lett 2013; 102: 062108
9. Zhang ZH, Huang Chen SW, Chu C, Tian K, Fang M, Zhang Y, Bi W, Kuo HC (2018) Nearly efficiency-droop-free AlGaN-based ultraviolet light-emitting diodes with a specifically designed superlattice p-type electron blocking layer for high mg doping efficiency. Nanoscale Res Lett 13:122
10. Zhang P, Li S, Liu C, Wei X, Wu Z, Jiang Y, Chen Z (2014) Near-infrared optical absorption enhanced in black silicon via ag nanoparticle-induced localized surface plasmon. Nanoscale Res Lett 9:519
11. Li D, Sun X, Jia Y, Stockman MI, Paudel HP, Song H (2017) Direct observation of localized surface plasmon field enhancement by Kelvin probe force microscopy. Light 6:e17038
12. Inoue SI, Naoki T, Kinoshita T, Obata T, Yanagi H (2015) Light extraction enhancement of 265nm deep-ultraviolet light-emitting diodes with over 90 mW output power via an AlN hybrid nanostructure. Appl Phys Lett 106: 131104
13. Li D, Jiang K, Sun X, Guo C (2018) AlGaN photonics: recent advances in materials and ultraviolet devices. Adv Opt Photon 10:43–110
14. Piprek J, Moe CG, Keller SL, Nakamura S, DenBaars SP (2004) Internal efficiency analysis of 280-nm light emitting diodes. Proc SPIE 5594:177
15. Gotoh H, Tawara T, Kobayashi Y, Kobayashi N, Saitoh T (2003) Piezoelectric effects on photoluminescence properties in 10-nm-thick InGaN quantum wells. Appl Phys Lett 83:4791
16. Bao G, Li D, Sun X, Jiang M, Li Z, Song H, Jiang H, Chen Y, Miao G, Zhang Z (2014) Enhanced spectral response of an AlGaN-based solar-blind ultraviolet photodetector with Al nanoparticles. Opt Express 22:24286
17. Li D, Sun X, Song H, Li Z, Chen Y, Jiang H, Miao G (2012) Realization of a high-performance GaN UV detector by nanoplasmonic enhancement. Adv Mater 24:845–849
18. Hirayama H, Enomoto Y, Kinoshita A, Hirata A, Aoyagi Y (2002) Efficient 230–280 nm emission from high-Al-content AlGaN-based multi quantum wells. Appl Phys Lett 80:37
19. Zhang JC, Zhu YH, Egawa T, Sumiya S, Miyoshi M, Tanaka M (2008) Influence of pulse width on electroluminescence and junction temperature of AlInGaN deep ultraviolet light-emitting diodes. Appl Phys Lett 92:191917
20. Zhang JC, Zhu YH, Egawa T, Sumiya S, Miyoshi M, Tanaka M (2008) Suppression of the subband parasitic peak by 1 nm i-AlN interlayer in AlGaN deep ultraviolet light-emitting diodes. Appl Phys Lett 93:131117
21. Zhang JC, Sakai Y, Egawa T (2010) Low-temperature electroluminescence quenching of AlGaN deep ultraviolet light-emitting diodes. Appl Phys Lett 96:013503
22. Schubert EF (2006) Light emitting diodes. Cambridge University Press, Cambridge

Submit your manuscript to a SpringerOpen journal and benefit from:

- ► Convenient online submission
- ► Rigorous peer review
- ► Open access: articles freely available online
- ► High visibility within the field
- ► Retaining the copyright to your article

Submit your next manuscript at ► springeropen.com